**Geomechanics and Engineering**, *Vol. 34, No. 5 (2023) 473-480*
https://doi.org/10.12989/gae.2023.34.5.473


# Mechanism of strength damage of red clay roadbed by acid rain

Guiyuan Xiao*[1,2], Jian Wang[1], Le Yin[3], Guangli Xu[2] and Wei Liu[4]

*[1]Key Laboratory of Geotechnics of Guangxi, Guilin University of Technology, Guilin, Guangxi 541004, China*
*[2]College of Engineering, China University of Geosciences, Wuhan, Hubei 430000, China*
*[3]Guangxi Zhuang Autonomous Region company of China National Tobacco Corporation 530000, China*
*[4]Shiyan City Natural Resources and Planning Bureau, Shiyan, Hubei 442099, China*

(*Received April 26, 2023, Revised Juen 14, 2023, Accepted June 23, 2023*)

**Abstract.** Acid rain of soils has a significant impact on mechanical properties. An X-ray diffraction test, scanning electron microscope (SEM) test, laser particle size analysis test, and triaxial unconsolidated undrained (UU) test were carried out in red clay soils with different compaction degrees under the effect of different concentrations of acid. The experiments demonstrated that: the dissolution effect of acid rain on colluvium weakened with the increase in the compacting degree under the condition of certain pH values, i.e., the damage to the structure of red clay soil was relatively light, where the number of newly increased pores in the soil decreased and the agglomeration of soil particles increased; for the same compacting degree, the structural gap decreased, and the agglomeration increased with the increase in the pH value (acidity decreases) of the acid rain; the dissolution rate of Si, Al, Fe, and other elemental minerals and cement in red clay soil was found to be higher under the effect of acid rain, in turn destroying the original structure of the soil body and producing a large number of pores. This is macroscopically expressed as the decrease of the soil cohesion and internal friction angle, thereby reducing the shear strength of the soil body.

**Keywords:** acid rain; red clay soils; roadbed diseases

## 1. Introduction

Most of the roads and railroads built in Guangxi are comprised of red clay (Wan *et al.* 2011). Currently, many scholars have conducted extensive research on the physical and mechanical properties of soils and have obtained good results (An *et al.* 2022, Guo *et al.* 2021, Jin *et al.* 2021).

The mechanical engineering properties of red clay soil are primarily determined by its material composition, structural characteristics, such as the microscopic pore distribution of red clay, chemical elements, etc. A large number of scholars have studied the nature of soil. Wei *et al.* (2022) established a structural soil shear zone extension model and verified it using experiments. They found that the thicknesses of the shear zone differed on macroscopic and microscopic scales, and the pore distribution, porosity, orientation, and anisotropy of the soil inside and outside the shear zone differed greatly. Madu (1977), Gidigasu (1972) and Ola (1980) investigated the relationship between sesquioxide the content and engineering properties from a microscopic perspective and found that the stress strain of the completed red clay foundation. Delage and Lefebvre (1984) and Dudoignon *et al.* (2001) performed an ontological analysis of the softening characteristics of the different types of red clays. Dafalla *et al.* (2022) investigated shear strength behaviour of compacted sand–clay mixtures used as liners.

At the same time, it is particularly important to study and assess the damage of acid rain on road foundations in areas with high incidences of acid rain where the natural environment is severely damaged (Zhang *et al.* 2023), considering that acid rain may lead to erosion of road foundations. Several scholars at home and abroad have conducted a large number of studies on soils under the action of pH. Gratchev and Towhata (2013) used a shear test to analyze the strength index of acidic materials in the soil. However, research on the mechanical indexes under acidic action is still lacking. Wang *et al.* (2021) and Cay (2023) considered the concentration of citric acid, flushing time and concentrations of Cu(II) and Pb(II) were considered to study the removal behaviors of heavy metals. In Bakhshipour *et al.* (2016) study, the effect of acid rain on the physico-chemical and microstructural properties of two different residual soils was investigated. Jahangir and Koupai (2020) considered water quality, particularly pH, is one of the most important factors that may significantly influence soil physical and mechanical properties leading to damage of structures. Hassanlourad *et al.* (2017) selected Mixture of sandy soil and bentonite clay to conduct a series of undrained triaxial tests. In this study, acid pollutant decreases the elastic modulus of the soil and increases the negative pore water pressure generated during shear. Liu *et al.* (2019) conducted the disintegration velocity was evaluated to investigate the effects of wetting-drying cycles and acid rain on soil disintegration characteristics.

In summary, this paper investigates the effect of acid rain on the shear strength of red clay from a microscopic perspective using SEM tests, agglomeration tests, and X-ray diffraction tests. The SEM maps obtained were further binarized and combined with the triaxial unconsolidated undrained (UU) test to fit the equation of the relationship

*Corresponding author, Professor
E-mail: xiaoguiyuangit@163.com



ISSN: 2005-307X (Print), 2092-6219 (Online)

Table 1 Basic physical and mechanical property indexes of the test soil samples

| Density /g·cm$^{-3}$ | Water content/% | Dry Density/g·cm$^{-3}$ | Specific Gravity | Liquid limit/% | plastic limit/% | Plasticity Index/$I_P$ |
|---|---|---|---|---|---|---|
| 1.65~1.74 | 26.85~31.5 | 1.3~1.33 | 2.76~2.78 | 61.3~71.2 | 34.2~38.4 | 31.5~36.8 |

Table 2 Roadbed compaction requirements

| Type of filling and excavation | Depth below the bottom of the road surface/m | Highways, primary roads (compaction degree/%) | Secondary road (compaction degree/%) | Third and fourth class roads (compaction degree /%) |
|---|---|---|---|---|
| Upper embankment | 0.80 ~ 1.50 | ≥94 | ≥94 | ≥93 |
| Lower embankment | 1.5 or less | ≥93 | ≥92 | ≥90 |

between the pore ratio and the shear strength under different concentrations of acid rain using power functions.

## 2. Test material preparation and test method

The soil was procured from the construction pit of the Guilin Ronghe Dijinghaoting project area (former Guilin Steel Factory) on Ludi Road, Guilin City, from a depth of approximately 5 m. The soil belongs to the Quaternary residual clay ($Q_4^{el}$), which is representative of the frequent occurrence of residual red clay in Guilin. The soil samples were tested according to the Highway Geotechnical Test Procedure (JTG 3430–2020), and the results are presented in Table 1.

### *2.1 Acid preparation*

Since the precipitation in China in the form of acid rain is of the sulfuric acid type, the main components of the test acid solution prepared for this experiment were sulfuric acid and nitric acid in a ratio of 3:1. The acid solution pH values were set to 3, 4 and 5. The acid solution of pH 3 was first prepared, followed by the preparation of acid solutions of pH 4 and 5 with a quantitative amount of distilled water. They were then compared with the standard solution (distilled water).

### *2.2 Test methodology*

The red clay soil sample was crushed and passed through a 0.5 mm sieve, mixed with the acid solution, to facilitate the pressing of triaxial specimens at a later stage, and to prevent the red clay from coagulating into large agglomerates during the mixing process as much as possible. After several tests, the initial moisture content of the pre-prepared soil samples was controlled at 23%. To simulate the compaction requirements of different roadbeds, soil samples of different compaction degrees and triaxial specimens with specifications of 39 mm×80 mm were prepared using the hydrostatic method with reference to the roadbed design specifications (JTGD30–2015), as presented in Table 2. The soil sample in acid solution was saturated for more than 7 days They were subsequently removed and weighed, and the saturation was calculated as per the relevant provisions of Section 4.7 of the Geotechnical Test Methods Standard. When the saturation was ≥ 95%, the unconsolidated undrained triaxial shear test was conducted as per the relevant provisions of Section 194 of the Geotechnical Test Methods Standard. The shear rate used was 0.8 mm/min. After the shear was completed, the sample was dismantled and dried, and the SEM test and agglomeration test were carried out on a portion of the soil sample under 200 kPa pressure. The SEM test was performed using the transmission electron microscope model 7582. Considering the chance nature of electron microscopy scanning tests, three parallel tests were conducted in each group, and the best test results were obtained through comparative analysis. The agglomeration test was also added, considering the uncertainty of the SEM test. After sieving through a 0.3 mm mesh, the soil sample was diluted into suspension in solution and put into the Winner 2008 particle size analyzer for testing. The three parallel groups were then set up for testing, and the average value was finally considered for analysis.

## 3. Test results and analysis

To analyze the effect of different acid rain concentrations on the shear strength of red clay with different degrees of compaction, the values of cohesion, internal friction angle under different acid concentrations, and compaction degrees were calculated based on triaxial tests, as presented in Figs. 1 and 2.

It may be observed from Figs. 1 and 2 that the shear strength of the remodeled soil gradually increased with the increasing compaction degrees. This is because, the interior of the soil sample is gradually compressed with increasing compaction, and the spacing between soil particles becomes smaller, thereby reducing the space for the soil particles to move and increasing the strength of the soil sample. This is expressed as an increase in the shear strength of the soil sample. Under a certain compaction condition, as the pH value of acid rain decreases (acidity increases), the structural gap of the red clay soil increases, and the connection ability between particles decreases. This is manifested as the decrease in the shear strength of soil samples.

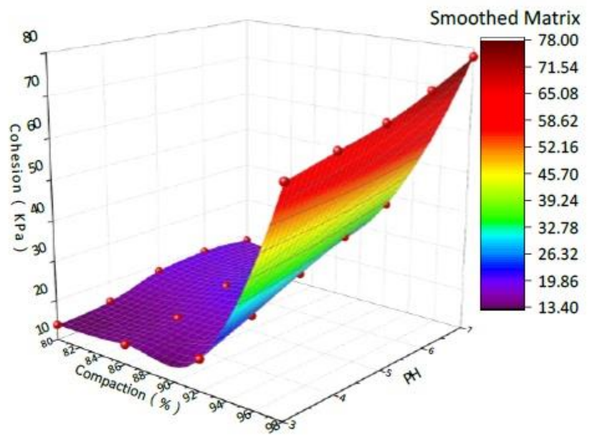


Fig. 1 Soil cohesion at different PH values and compaction levels

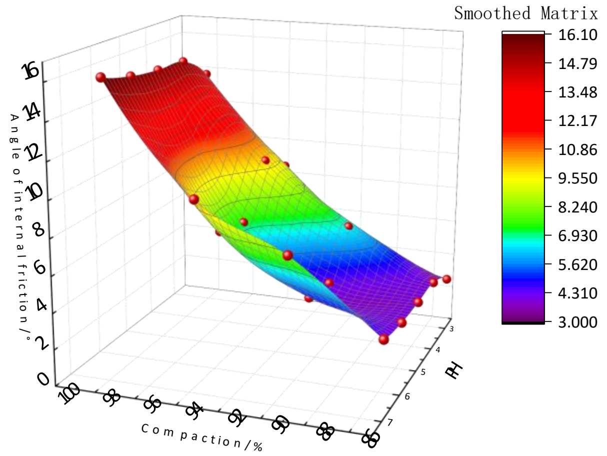


Fig. 2 Friction angle within the soil at different PH values and compaction levels

Further, to quantify the shear strength index of the different soil samples, According to Fig. 1, Fig. 2 was fitted to derive the spatial surface equations of cohesion and the internal friction angle of red clay soils subjected to different concentrations of acid rain and compaction degrees. The fitting Eq. (1) is shown below.

$$\begin{cases} C = 1896.58418 - 45.31198 * PH + 6.25864 * b + 0.26931 * PH - 0.28409 * b \\ \varphi = 321.14267 - 7.73062 * PH - 0.24427 * b + 0.0496 * PH + 0.06318 * b \end{cases} \quad (1)$$

where C is the cohesive force of soil, φ is the angle of internal friction, and b is the compaction degree of soil.

From Eq. (1), it may be observed that the cohesive force decreases significantly with increasing acid strength, where the greater the compaction degree, the greater the decrease of the cohesive force of the soil. When the acidic strength is small, the internal structure of the red clay is less destroyed by acid, and the association force is less reduced, which indicates that the cohesion is larger and the shear strength is higher. As the acidic strength increases, the material between the soil particles inside the red clay is gradually destroyed, and the soil particles are gradually separated, thereby gradually reducing the association strength. This indicates that the cohesion is reduced, and the shear strength of the soil is lower.

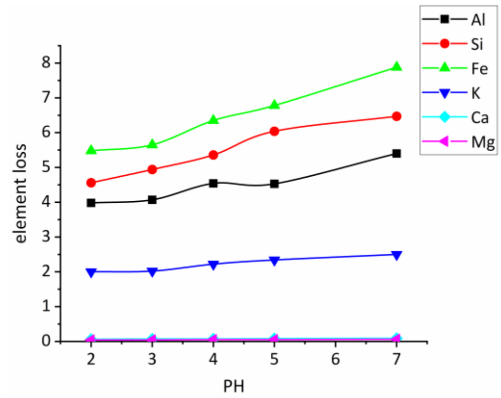


(a) elements loss

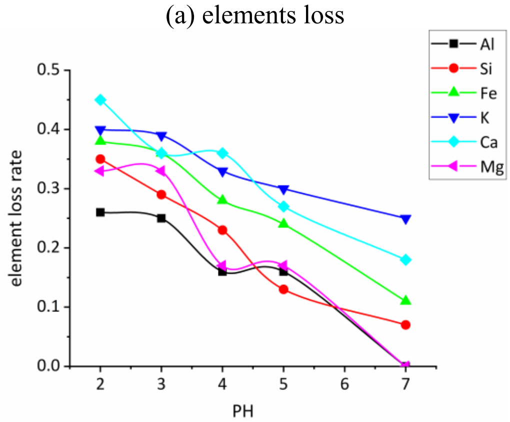


(b) elements loss rate

Fig. 3 Graph of element loss after different pH solutions

### *3.1 Analysis of ion mobility*

To verify the erosive effect of acid on red clay, the elemental mass fraction of red clay was tested using X-ray fluorescence spectroscopy analysis before and after contamination, followed by the calculation of the elemental loss rate. Fig. 3 demonstrates the change curves of the mass fraction of some elements and the element loss rate in the red clay at different pH.

From the red clay elemental content versus pH curves in Fig. 3, it is clear that the content of elemental iron, elemental aluminum, elemental silicon, and elemental magnesium decreased with decreasing solution pH (increasing acidity). This may be due to the dissolution of various chemical components in the red clay by the acid, resulting in irreversible damage to the internal integrity of the soil sample. The element loss rate of red clay soaked in different solutions demonstrated the following pattern: as the pH of the solution increased (acidity decreased), the loss rate of various elements in red clay post soaking in acid demonstrated a linearly decreasing trend. The loss rate of the four main test elements in an acidic environment was determined to be in the order of Mg<Si<Al<Fe, with the loss rate of each main element of red clay in an acid rain

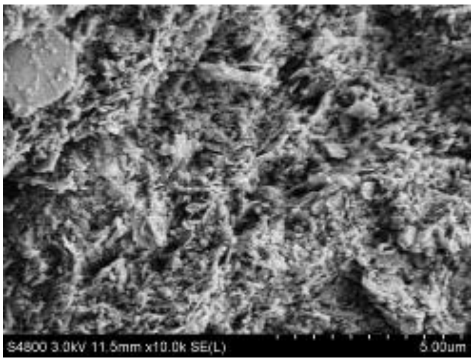


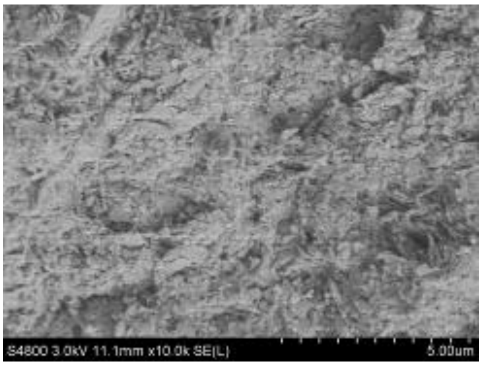


(a) 85% compaction (b) 98% compaction

Photographs of remodeled soil with pH 5

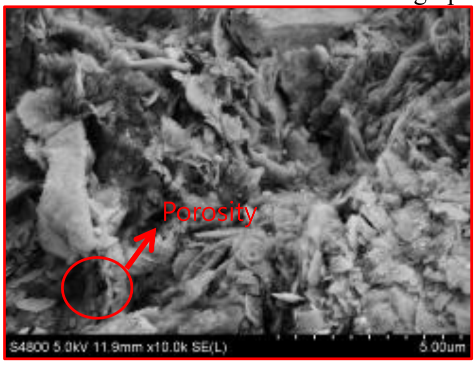


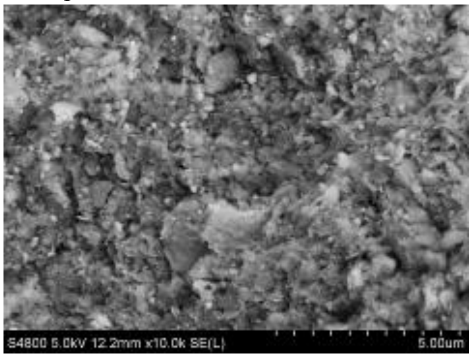


(c) 85% compaction (d) 98% compaction

Photographs of remodeled soil with pH 3

Fig. 4 Electron microscope scans of remodeled red clay at different compaction levels with different acid drenching

environment of pH 2 being the largest, thereby indicating that acid rain has a strong dissolving effect on red clay. The content of Si, K, and Fe decreased slightly after soaking in water, among which the elemental content of Fe decreased the most, and that of Mg changed only slightly. This shows that the compounds of K are insoluble in water, while Si, Al, and Fe can be partially soluble in distilled water.

According to Wang Jing *et al*. (2019), it was found that the cohesion of the soil is primarily affected by $Fe_2O_3$, etc., and the internal friction angle is determined by the minerals containing Si, Fe and Al primarily exist in the form of colloids, whose chemical reactions are presented in Eq. (2).

These colloids are easily eroded by acid dissolution under acidic conditions, resulting in the destruction of the link structure between soil particles and a reduction in soil cohesion.

$$\begin{aligned} Fe_2O_3 + 6H^+ &= 2Fe^{3+} + 3H_2O \\ Al_2O_3 + 6H^+ &= 2Al^{3+} + 3H_2O \end{aligned} \tag{2}$$

In terms of Si, which is primarily present in kaolinite. When it is contaminated with acid, the chemical reaction can be given as Eq. (3). The more acidic the environment, the more the minerals are dissolved and eroded, thereby resulting in a decrease in the internal friction angle of the clay.

$$Al_2Si_2O_5(OH)_4 + 6H^+ = 2Al^{3+} + 2H_4SiO_4 + H_2O \tag{3}$$

### *3.2 Microstructural analysis of red clay*

Further SEM tests were conducted to assess the reasons for the reduction of red clay by acid rain erosion at different compaction levels. Due to the limited space, only the electron microscope scans of red clay soils with 85% and 98% compaction under the effect of acid rain at pH 3 and 5 were considered for comparative analysis. It was found that the surface pores of the red clay soil specimens that had been soaked in an acidic solution pH were more porous, the soil particles were finer, the pores were denser, and the pores were deeper. On the other hand, the pores of red clay soils soaked with distilled water also demonstrated certain changes, with the pores becoming larger and the soil particle being reduced.

In this study, the SEM image was converted into a binary image using Image-Pro Plus software (Fig. 4), where the white indicates the pore space and the black the soil matrix, this is the best result determined by segment debugging. The IPP software is analysed using a pixel classification algorithm. The pores and the whole image were then labeled using IPP software to obtain the number of pixels in the pores and the complete image. The pore ratio of the remodeled soil was then calculated.

According to the test photos, binarization diagrams, and pore distribution diagrams presented in Figs. 4-6, it was found that the acid rain electron micrographs of the remodeled red clay soil under pH 3, 4, and 5 and different compaction degrees (85%, 90%, 95%, and 98%) demonstrated that the greater the compaction degree, the

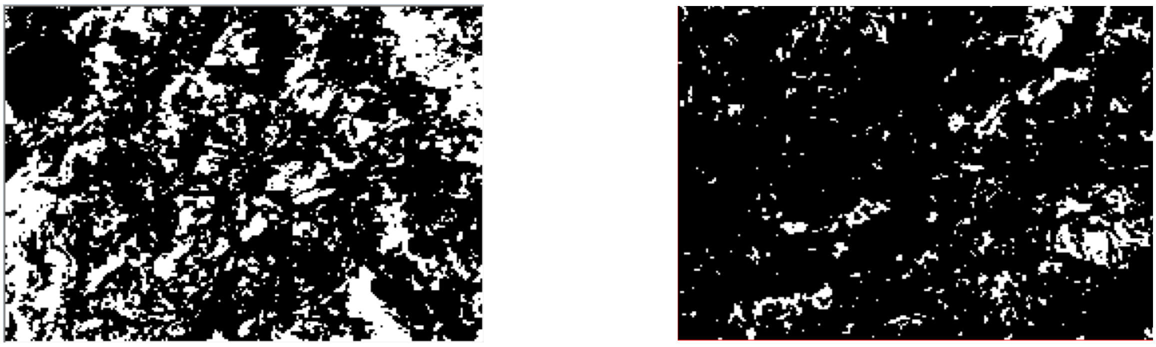

(a) 85% compaction (b) 98% compaction
Binarization diagram of remodeled soil with pH 5

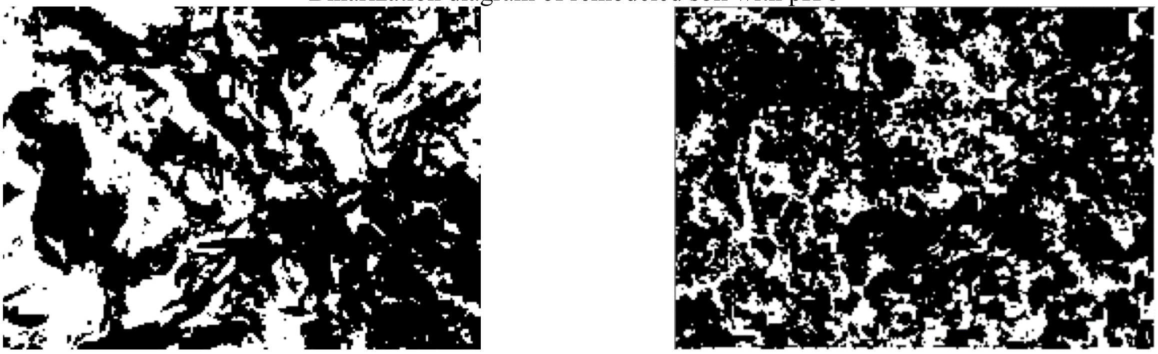

(c) 85% compaction (d) 98% compaction
Binarization diagram of remodeled soil with pH 3

Fig. 5 Binarization diagram of remodeled red clay with varying compaction degrees under different concentrations of acid drenching

larger the structural agglomerate particles and lesser the visible number of pores. On the other hand, it was observed that with a smaller compaction degree, the red clay soil body in the soil specimens demonstrated more pores on the surface, the soil particles were finer, and the pores are denser and deeper.

In the same compaction, the electron microscope images of the remodeled red clay with simulated acid rain drenching of pH 5 demonstrated that the structural agglomerate particles were relatively large and dense, and the size and the visible number of pores were relatively small. The surface of the remodeled red clay soil specimens soaked in an acid solution of pH 3, on the other hand, demonstrated a greater number of pores which were denser and deeper, with finer soil particles. Uncontaminated red clay surface was found to be smoother. In general, it may be deduced that by reducing large particles in the soil, the inter-particle pores and the number of pores gradually increase, and the soil becomes loose and porous with the increase of acid concentration (pH value becomes smaller).

In the case of a certain pH value, with the increase in compaction, it was observed that the large particles in the soil body increased and were held together, and the inter-particle pores were found to be relatively less. The lesser the acid solution penetrated the interior of the red clay specimen, the lesser the erosion of the soil body, with significantly lesser pore damage.

From the pictures of the SEM, a large number of pores were observed between the soil grains, especially in the case of pH 4. The structure of the red clay soil became brittle and loose, and that of the soil body became poor, resulting in cracks on the surface of the soil sample and an increase in the number of pores. The structure of red clay soil was relatively dispersed under the effect of acid rain, where the original agglomerates got dismantled, and ion dissolution loss caused the internal pores to become larger. Erosion of the soil body by the acid led to the dissolving and subsequent loss of the linkage or cement between the structures. The red clay soil interior was subsequently loose and porous, the pore ratio increased, the degree of compactness lessened, the friction between the clay particles weakened, and the clumping effect reduced.

The red clay microstructure is composed of agglomerates of aggregated grains. The particle-to-particle contact is primarily face-to-face, with the presence of iron and other elements on the particle surface. The agglomerates and agglomerate structures between the particles constitute the macroclay body through the cementation of iron-aluminum cement. Under the action of a strong acid, these colloids are dissolved and eroded.

The dissolution effect of acid rain on red clay soil is the outcome of the chemical interaction of sesquioxides with acid. The original structure of the soil is destroyed, and the cementation link between the agglomerates is lost. The macroscopic manifestation of this is the damaging effect of the shear strength of the red clay soil body. From the aforementioned electron microscope pictures, it may be deduced that the more acidic the rain, the more obvious the pores of the soil, thereby proving that the more intense the soil damage, the more the reduction in the shear strength of the soil.

Table 3 Test results of the microagglomerates of primary red clay under different pH conditions

| | pH = 3 | pH = 4 | pH = 5 | pH = 7 |
|---|---|---|---|---|
| >0.002 mm Microagglomerates | 80.3% | 83.71% | 84.62% | 90.78% |
| >0.005 mm Microagglomerates | 51.2% | 52.31% | 57.66% | 68.56% |
| >0.01 mm Microagglomerates | 15.6% | 22.31% | 25.24% | 44.17% |
| Reunion degree | 11.82% | 14.89% | 21.64% | 32.81% |

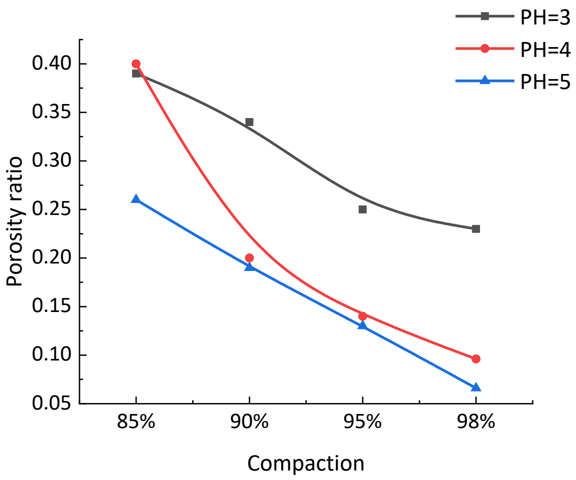


Fig. 6 Pore distribution of remodeled red clay at different compaction degrees with different acid drenching

The acid causes the loss of cementing material between the mineral agglomerates of the red clay, thereby increasing the distance between the molecules of the mineral agglomerates and decreasing the attraction, and to some extent, also decreasing the cohesion of the red clay.

### *3.3 Analysis and results of the agglomeration test*

Due to the limitations of the SEM test, the lack of clarity of the pictures led to difficulties in clear discrimination during the analysis. This test was therefore supplemented with a particle agglomeration test to obtain the desired conclusion.

The agglomeration degree was calculated as follows.

Soil agglomeration condition was calculated using the formula: $X_1 = n_1 - n_2$ where $n_1$ is the analytical value of >0.05 mm microagglomerates and $n_2$ is the analytical value of >0.05 mm particle composition.

Soil agglomeration calculation formula: $X_2 = X_1/n_1 \times 100\%$ where $X_2$ is the soil agglomeration analysis value, $X_1$ is the agglomeration condition, and $n_1$ is >0.05 mm microagglomerate analysis value.

The results of laser particle size analysis of red clay under different acidic conditions are presented in Table 3. With the gradual increase in solution pH, the proportion of large particle size in red clay soil particles gradually increases, along with the agglomeration degree. The greater the acidic strength of the solution, the more the decomposition of the soil particles in the red clay into small particle sizes, the more the large agglomerates are decomposed under the action of acid dissolution, and the smaller the agglomeration of the soil sample, resulting in the reduction of the shear strength.

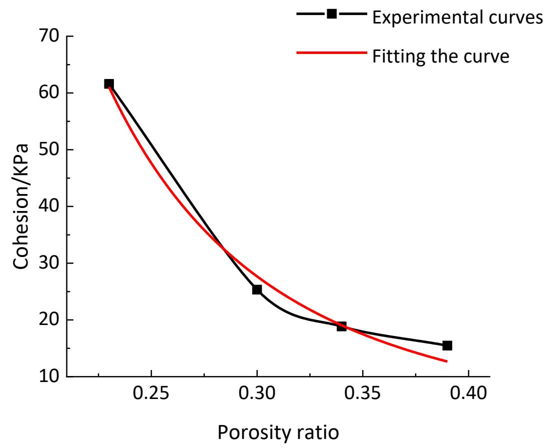


Fig. 7 Fitting curve

Table 4 Parameters for cohesive porosity curve fitting

| pH | a | b | $R^2$ |
|---|---|---|---|
| 3 | 0.76637 | -2.97871 | 0.98995 |
| 4 | 3.27867 | -1.2541 | 0.96749 |
| 5 | 6.38309 | -0.88118 | 0.94447 |

Table 5 Internal friction angle, porosity curve fitting parameters

| pH | a | b | $R^2$ |
|---|---|---|---|
| 3 | 1.14878 | -1.02757 | 0.94091 |
| 4 | 3.17084 | -0.50462 | 0.98386 |
| 5 | 7.42199 | -0.24364 | 0.94266 |

### *3.4 The relationship between pore ratio and shear strength*

To quantitatively describe the relationship between microstructure and shear strength. The relationship equation between porosity and shear strength was fitted using power function with reference to the method of Yang *et al.* (2019) and others in the study on the shear resistance model of Yan'an loess. A schematic diagram of the fitting curve analyzed in this paper is presented in Fig. 7. Only the fitting curve plot for pH 3 is listed in this paper, and the fitting parameters for the rest of pH are presented in Tables 4 and 5.

The relationship between porosity and shear strength for different pH and different compaction degrees may be obtained by substituting the fitted parameters in Tables 4 and 5 into Eq. (4).

$$\tau_f = c + \sigma tan\varphi \tag{4}$$

where $\tau_f$ is the shear strength.
c is the cohesive force of the soil, g-cm$^{-3}$.
σ is the normal pressure on the shear-damaged surface.
φ is the angle of internal friction of the soil.

$$\begin{cases} \tau_f = 0.76637n^{-2.97871} + tan(1.14878n^{-1.02757}) \cdot \sigma, & PH = 3 \\ \tau_f = 3.27867n^{-1.2541} + tan(3.17084^{-0.50462}) \cdot \sigma, & PH = 4 \\ \tau_f = 6.38309n^{-0.88118} + tan(7.42199n^{-0.24364}) \cdot \sigma, & PH = 5 \end{cases} \tag{5}$$

where n is the pore ratio.

It may be observed from Eq. (5) that the shear strength decreased significantly with the increase of acid strength. The larger the pore ratio, the greater the cohesion of the soil, and the greater the decrease of the angle of internal friction. When the acidic strength is small, the internal structure of the red clay is less destroyed by acid, and the linkage force decreases, indicating a larger cohesive force and higher shear strength. As the acidic strength increases, the material between the soil particles inside the red clay is gradually destroyed, and the soil particles are gradually separated, i.e., the pore ratio of the soil body becomes larger, the linkage strength gradually decreases, and the soil particles become more dispersed. This indicates that the cohesive force and the internal friction angle decrease, eventually leading to a decrease in the shear strength of the soil body.

## 4. Conclusions

1. An increase in the acidic strength of the solution under a certain degree of compaction led to an increase in the decomposition of the soil particles in the red clay into small particle sizes by the action of acid. Large agglomerates were further decomposed under the action of acid dissolution and corrosion. It was observed that the lower the agglomeration of the soil sample, the more the loss of chemical element components, ultimately resulting in smaller shear strength.
2. Under the condition of a certain pH value, the damage to the soil body was weakened as the compaction of red clay increased. The dissolution effect of the acid rain on the cement decreased, thereby weakening the damage to the red clay soil structure and reducing the number of pores produced. The individual pores were found to be small, and the agglomeration of the soil sample increased, with a decrease in the amount of chemical element loss, thereby resulting in greater shear strength.
3. In this paper, a power function is fitted to the test data to obtain an equation for the shear strength of soils under acidic conditions.

## Acknowledgements

The authors thank Mr. Yukai fang for assisting with the SEM measurements.

## Disclosure statement

No potential conflict of interest was reported by the author(s).

## Funding

This research is sponsored by Natural Science Foundation of China [grant number 52169022]

## References

An, R., Kong, L., Zhang, X. and Li, C. (2022), “Effects of dry-wet cycles on three-dimensional pore structure and permeability characteristics of granite residual soil using X-ray micro computed tomography”, *J. Rock Mech Geotech Eng*., **14**(3), 851-860. https://doi.org/10.1016/j.jrmge.2021.10.004.

Bakhshipour, Z., Asadi, A., Huat, B.B., Sridharan, A. and Kawasaki, S. (2016), “Effect of acid rain on geotechnical properties of residual soils”, *Soils Found.*, **56**(6), 1008-1020. https://doi:10.1016/j.sandf.2016.11.006.

Cay S. (2023), “Assessment of tea saponin and citric acid-assisted phytoextraction of Pb-contaminated soil by Salvia virgata Jacq”, *Environ. Sci. Pollut. Res. Int*., **30**(17), 49771-49778. https://doi:10.1007/S11356-023-25809-9.

Dafalla, M., Shaker, A., Elkady, T., Almajed, A. and Al, S.M. (2020), “Shear strength characteristics of a sand clay liner”, *Sci. Rep.,* **10**(1), 18226. https://doi:10.1038/s41598-020-75188-1.

Delage, P. and Lefebvre, G. (1984), “Study of the structure of a sensitive Champlain clay and of its evolution during consolidation”, *CA Geotech. J.*, **21**(1), 21-35. https://doi.org/10.1139/t84-003.

Dudoignon, P., Pantet, A., Carrara, L. and Velde, B. (2001), “Macro–micro measurement of particle arrangement in sheared kaolinitic matrices”, *Géotechnique*, **51**(6), 493-499. https://doi.org/10.1680/geot.2001.51.6.493.

Gidigasu, M.D. (1972), “Mode of formation and geotechnical characteristics of laterite materials of Ghana in relation to soil forming factors”, *Eng. Geol.*, **6**(2), 79-150. https://doi.org/10.1016/0013-7952(72)90034-8.

Gratchev, I. and Towhata, I. (2013), “Stress–strain characteristics of two natural soils subjected to long-term acidic contamination”, *Soils Found.*, **53**(3), 469-476. https://doi.org/10.1016/j.sandf.2013.04.008.

Guo, Y., Ni, W. and Liu, H. (2021), “Effects of dry density and water content on compressibility and shear strength of loess”, *Geomech. Eng.,* **24**(5), 419-430. https://doi.org/10.12989/gae.2021.24.5.419.

Hassanlourad, M., Khatami, M.H. and Ahmadi, M.M. (2017), “Effects of sulphuric acid pollutant on the shear behaviour and strength of sandy soil and sand mixed with bentonite clay,” *Int. J. Geotech. Eng.*, **11**(2), 114-119. https://doi:10.1080/19386362.2016.1193662.

Jahangir, A, and Koupai, M. (2020), “Effect of pore water pH on mechanical properties of clay soil”, *Bull. Eng. Geol. Environ.*, **79**(1), 1461-1469. https://doi:10.1007/s10064-019-01611-1.

Jin, P., Zhen, W., Chen, B., Sun, D.A., Gao, Y. and Xiong, Y. (2021), “Effect of microstructure on water retention behavior of lateritic clay over a wide suction range”, *Geomech. Eng.,* **25**(5), 417-428. https://doi.org/10.12989/gae.2021.25.5.417.

Liu W., Song, X., Huang, F. and Hu, L. (2019), “Experimental study on the disintegration of granite residual soil under the combined influence of wetting–drying cycles and acid rain”, *Geomat. Nat. Hazards Risk*, **10**(1), 1912-1927.

https://doi:10.1080/19475705.2019.1651407.
Madu, R.M. (1977), “An investigation into the geotechnical and engineering properties of some laterites of Eastern Nigeria”, *Eng. Geol.*, **11**(2), 101-125. https://doi.org/10.1016/0013-7952(77)90022-9.
Ola, S.A. (1980), “Mineralogical properties of some nigerian residual soils in relation with building problems”, *Eng. Geol.*, **15**(1), 1-13. https://doi.org/10.1016/0013-7952(80)90027-7.
Wan, Z., Guo, A. and Tan, Y. (2011), “Research on filling technologyof red clay embankmet in southwest Hunan”, *Geotech. Mech.*, **32**(8), 2281-2286. https://doi.org/10.4028/www.scientific.net/AMR.291-294.2281.
Wang, J., Lv, X. and Qu, X. (2019a), “Relationship between shear strength of roadbed soils and chemical and mineral composition”, *J. Jilin Univ. (Eng. Ed.)*, **49**(3), 766-772.
Wang, Y., Tang, L. and Liu, L. (2021), “Removal behaviors of Cu and Pb from heavy metal contaminated silts flushed by citric acid”, *Geomech. Eng.*, **26**(5), 489-497. https://doi.org/10.12989/gae.2021.26.5.489.
Wei, Y.Z., Yao, Z.H., Chong, X., Zhang, J.H. and Zhang, J. (2022), “Microstructure of unsaturated loess and its influence on strength characteristics”, *Sci. Rep.*, **12**(1), 1502. https://doi:10.1038/S41598-022-05464-9.
Yang, Z., Ding, P. and Yu, D. (2019), “Shear strength model of Yan'an loess based on porosity”, *J. Mountain Sci.*, **37**(3), 392-399.
Zhang, Y., Li, J. and Tan, J. (2023), “An overview of the direct and indirect effects of acid rain on plants: Relationships among acid rain, soil, microorganisms, and plants”, *Sci. Total Environ.*, **873**, 162388. https://doi:10.1016/J.SCITOTENV.2023.162388.

*GC*